

Quantum Chaos of a Kicked Particle in an Infinite Potential Well

Bambi Hu,^{1,2} Baowen Li,¹ Jie Liu,^{1,3} and Yan Gu^{1,4}

¹*Department of Physics and Centre for Nonlinear Studies, Hong Kong Baptist University, Hong Kong, China*

²*Department of Physics, University of Houston, Texas 77204-5506*

³*Institute of Applied Physics and Computational Mathematics, P.O. Box 8009, Beijing 100088, China*

⁴*Center for Fundamental Physics, University of Science and Technology of China, Hefei, China*

(Received 26 October 1998)

We study quantum chaos in a non-KAM system exemplified by a particle in an infinite potential well subject to a periodic kicking force. For a small perturbation K , the classical phase space displays a stochastic web structure, and the diffusion coefficient scales as $D \propto K^{2.5}$. However, in the large K regime, $D \propto K^2$. Quantum mechanically, we observe that the level spacing statistics of the quasideigenenergies changes from Poisson to Wigner distribution as K increases. The quasideigenstates are power-law localized for small K and extended for large K . Possible experimental realization of this model is also discussed. [S0031-9007(99)08900-0]

PACS numbers: 05.45.Mt, 03.65.Sq

In the study of quantum chaos, most works have been concentrated on quantum systems whose classical counterparts obey the Kolmogorov-Arnold-Moser (KAM) theorem. In such systems, as the external or driven parameter is increased, the invariant curves gradually break up. Local chaos evolves into global chaos and diffusion takes place. The widely studied models are the kicked rotator (KR) [1,2] and quantum billiards [3]. In these models, a conspicuous phenomenon is dynamical localization, namely, the quantum suppression of classical diffusion. This phenomenon was discovered numerically by Casati *et al.* [1] in the KR, and later confirmed by several experiments such as a Rydberg atom in a microwave field [4] and an atom moving in a modulated standing wave, etc. [5]. This phenomenon has been found to be generic not only in the kicked quantum systems but also in conservative Hamiltonian systems such as quantum billiards [6], the Wigner band random matrix model [7], and a single ion confined in a Paul trap [8].

However, besides the systems mentioned above, there exists another class of systems which is non-KAM. In these systems, the invariant curves do not exist at all for any small external or driven parameters. Compared with the KAM systems, much less is known about quantum chaos in such systems. For instance, we have only limited knowledge of the kicked harmonic oscillator (KHO) introduced by Zaslavsky *et al.* [9,10] to describe a charged particle moving in a magnetic field and under the disturbance of a wave packet. This model can also be used to describe a single ion trapped in a harmonic potential [11]. This system is a degenerate one and does not satisfy the KAM theorem. It is difficult to study quasideigenenergies, quasideigenstates, and long time diffusion of this model [12] because its phase space is unbounded and cannot be reduced to a cylinder, as in the case of the KR.

The purpose of this Letter is twofold: (1) to construct a simple non-KAM system which could be investigated

numerically both classically and quantum mechanically; (2) to study quantum chaos in such a system. As we shall see, despite its simplicity, our model shows a stochastic web structure in the classical phase space. Unlike the KHO, the quasideigenenergies and quasideigenstates of this model can be computed easily. Furthermore, like the KR, our model might be realized experimentally. The study of this model aims to enrich our understanding of quantum chaos in non-KAM quantum systems.

The model we consider in this Letter is a particle moving inside a one-dimensional (1D) infinite square potential well and under the influence of a kicked periodic external potential. The difference of this model from the KHO lies in its phase configuration. As mentioned before, the phase space of the KHO is unbounded both in coordinate and momentum, whereas it is bounded on a cylinder with flattened end in our model.

The Hamiltonian of our model is given by

$$H = \frac{p^2}{2} + V_0(q) + k \cos(q + \alpha) \sum_{n=-\infty}^{\infty} \delta(t - nT), \quad (1)$$

where

$$V_0(q) = \begin{cases} \infty, & \text{for } q = 0, \pi \\ 0, & \text{elsewhere,} \end{cases}$$

and α is a phase shift. Our model is a modification of the KR. There are, however, two minor changes: (1) Two hard walls are set up at $q = 0$ and π , respectively; and (2) a phase shift α for the potential is introduced. In this Letter, we take $\alpha = 1$ for illustrative purposes; no essential difference is found for other values of α . The two hard walls destroy the analyticity of the potential, hence non-KAM. The phase shift breaks the parity symmetry.

Classical dynamics.—The main characteristic of this system is the existence of stochastic webs in the classical phase space. Thus diffusion can take place along the

stochastic webs for any small K ($= kT$); see, e.g., Fig. 1. This is a fundamental difference from a KAM system like the KR. In the KR, for any $K < K_c = 0.971635\dots$, no global diffusion occurs due to the existence of invariant curves. The properties of the stochastic webs such as the thickness and symmetry, etc., are also very interesting [9]. We will, however, leave this work to future investigations. As K increases, the stochastic layer becomes wider and wider, and eventually covers the whole phase space. In calculating the diffusion coefficient for a given K , we have taken 10^4 points starting from stochastic regions, and all the initial trajectories evolve for one million periods. Averages are taken over 10^4 trajectories for each time period. It is found that the energy diffusion is asymptotically linear for all values of K .

The diffusion coefficient D ($\equiv \langle E_n \rangle / n$) as a function of K is plotted in Fig. 2. It is evident that there exist two different diffusion regions. For $K \gg 1$, $D \sim K^2$, whereas for $K \ll 1$, $D \sim K^{2.5}$, which is similar to that of the discontinuous twist map [13]. However, the underlying mechanism is quite different. In the case of the discontinuous twist map, the superslow diffusion is caused by the stickiness of the cantori, whereas in our model it is due to the stable islands.

Now we turn to the quantum behaviors of this model. One may ask: How do such classical characteristics as stochastic webs and superslow diffusion manifest themselves in the quantum statistics of quasieigenenergies and quasieigenstates? This is a very interesting question in the study of quantum chaos. Since our model is a periodically driven system, the evolution operator over one period T of the kick is given by $\hat{U}(T) = \exp(-\frac{i\hat{p}^2 T}{4\hbar}) \exp(-\frac{iV(\hat{q})}{\hbar}) \exp(-\frac{i\hat{p}^2 T}{4\hbar})$,

where $V(q) = k \cos(q + \alpha)$. The operator $\hat{U}(T)$ is also called the Floquet operator, and it is time-reversal invariant. Moreover, it is unitary and satisfies the eigenvalue equation, $\hat{U}(T)|\Psi_\lambda\rangle = e^{-\frac{i\lambda}{\hbar}}|\Psi_\lambda\rangle$ where the phase λ is real. λ/T is the quasieigenenergy, and Ψ_λ the quasieigenstate (or the Floquet state).

The quasieigenenergies can be obtained by diagonalizing $\hat{U}(T)$ within a large number of bases $|n\rangle$, which we choose as the eigenstates of the nonperturbed Hamiltonian, $\langle q|n\rangle = \sqrt{2/\pi} \sin(nq)$, $q \in [0, \pi]$; $n = 1, 2, \dots, N$. In our calculations N is kept at 1024 [the calculation is also performed with 512 bases, but no qualitative or quantitative difference is found]. The elements of the operator U are $U_{nm} = \langle n|\hat{U}(T)|m\rangle$. As $\hat{U}(T)$ is a unitary operator, we can define a Hermitian operator $\hat{C} = \frac{1}{2}[\hat{U}(T) + \hat{U}^\dagger(T)]$. Then the matrix elements C are $C_{nm} = A_{nm} + iB_{nm}$. The matrices \mathbf{A} and \mathbf{B} satisfy the condition $\mathbf{A}^T = \mathbf{A}$ and $\mathbf{B}^T = -\mathbf{B}$, respectively.

$\begin{bmatrix} \mathbf{A} & -\mathbf{B} \\ \mathbf{B} & \mathbf{A} \end{bmatrix}$ is a $2N \times 2N$ symmetric matrix. The standard algorithm [14] is used to diagonalize the above matrix to obtain the eigenvalues and eigenvectors $[u, v]$. We project the N dimensional vector $(u + iv)$ onto the basis of a plane wave to obtain the eigenstates of $\hat{U}(T)$. The fast Fourier transform (FFT) of sinusoidal form [14] is employed to transform the wave function between the position representation and the energy representation.

Quasieigenstates.—The quasieigenstates show behaviors quite different from that of the KR. In the KR, the quasieigenstates are exponentially localized in the momentum space [2]. In our model, however, the quasieigenstates are power-law localized, as shown in

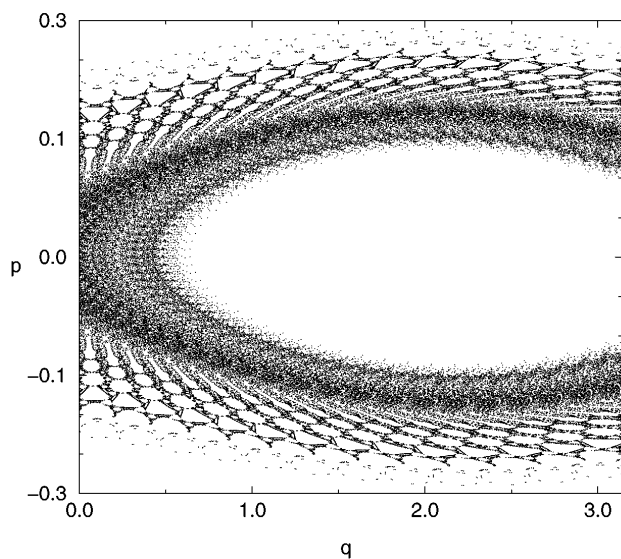


FIG. 1. A typical classical phase space of our model at very small perturbation strength. The stochastic web structure is clearly seen. Here we have $K = 0.01$, $\alpha = 1$. One trajectory starts from $(q_0 = 0.1, p_0 = 0.012)$ and evolves for 10^5 periods.

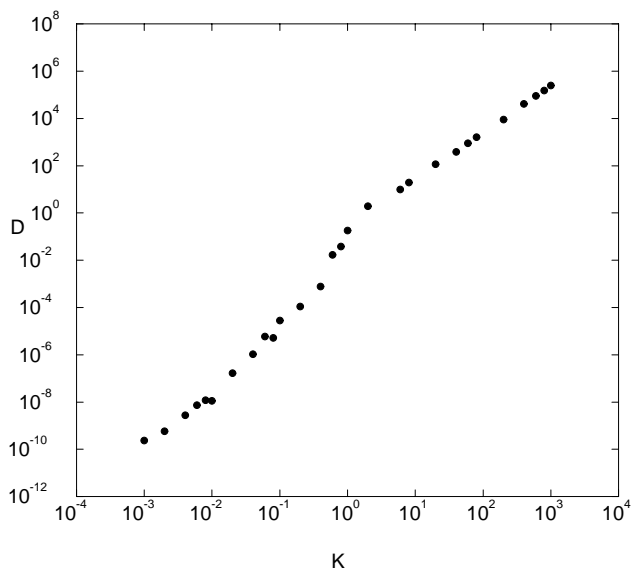


FIG. 2. Classical diffusion coefficient D versus perturbation strength K . The best fit by using the data $K > 1$ gives rise to a slope 1.97, whereas that by using the data $K < 0.1$ gives rise to a slope 2.47. A clear turning point of the slope can be seen at K about 1.

Fig. 3. In this figure, we demonstrate a few typical states at different values of K for localized, intermediate, and extended ones, respectively. It is clearly seen that the localized states gradually transit to extended ones as we increase K . This transition, as we shall see later, will also manifest itself in the statistics of quasieigenenergies.

In fact, the power-law localization of the eigenstates is traceable to the structure of the matrix U . In the KR, the matrix elements $U_{m,m+n}$ decay faster than exponential when n exceeds the band width b , which is proportional to K . Thus the elements outside this band can be regarded as effectively zero. Within the band of width b , the elements are pseudorandom [2]. This kind of band random matrix has attracted much interest. However, in our model the situation is different. A careful analysis shows that the elements outside the band decay as a power law with $|U_{m,m+n}| \approx 1/n^2$. We have calculated $\langle U^2 \rangle_n (\equiv \langle U_{m,m+n}^2 \rangle_m)$ for four different K 's, and plot them in Fig. 4. The typical slope of the curves over a large range is approximately -4 . The band width b in our model is found to scale as $b \propto K$. Inside this band the magnitude of the matrix elements is almost a constant. This kind of band random matrix describes a new class of physical systems, such as systems with nonanalytic singular boundary [15].

Statistics of quasieigenenergies.—The structure of the quasieigenstates determines the energy level statistics. As is well known, level repulsion can occur between the Floquet eigenvalues when the Floquet eigenfunctions overlap. In the KR, the quasieigenfunctions are exponentially localized in angular momentum. Since angular momentum has a finite range, the Floquet states with very close eigenvalues may lie so far apart that they don't overlap. Thus, we don't have any level repulsion for these two eigenvalues. This is the reason why Poisson-like spectral statistics persists in the KR even though the system is

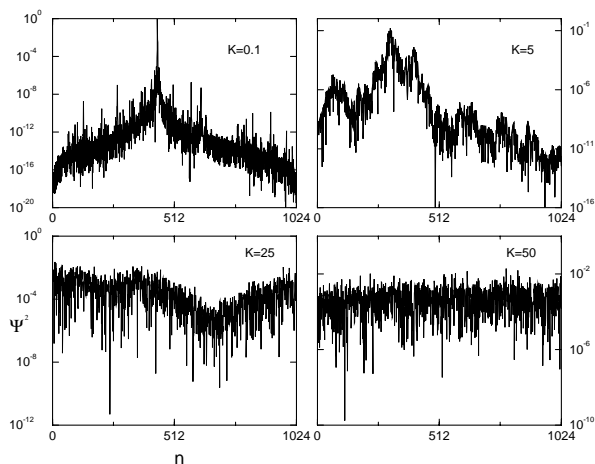


FIG. 3. Typical quasieigenstates in these different regimes: localized ($K = 0.1$ and 5), intermediate ($K = 25$), and extended ($K = 50$). The corresponding values of K are shown in the figure.

classically chaotic. To observe the transition from Poisson to Wigner distribution, one has to consider the KR defined on a torus [2].

In our model, however, the Floquet states do overlap in momentum space, as is shown above. Therefore, we expect to observe the transition of the quasieigenenergies statistics. The level spacing statistics of the quasieigenenergies is shown in Fig. 5 for four different values of $K = 0.1, 5, 25,$ and 50 . This figure demonstrates a smooth transition from Poisson to Wigner distribution. To quantify this transition, the Brody distribution [16] is used to best fit the above four distributions. [In fact we use the cumulative distribution function $I(s) = \int_0^s P(s') ds'$.] The best fit gives rise to the Brody parameter $\beta = 0.03, 0.08, 0.46,$ and 0.82 for the four distributions shown in Fig. 5. To check the approach to Poisson distribution as K decreases to zero, $P(s)$ is also calculated for $K = 10^{-4}$. As expected, we obtain a good Poisson distribution. The best fit gives $\beta = 0.01$.

It should be pointed out that the origin of difference between our model and the KR comes from nonanalyticity of the potential. This makes the phase space in our model a half cylinder with the end flattened. This nonanalyticity also leads to a different structure of the evolution matrix U . Moreover, the model considered here is of more than academic interest. An experimental realization of the KR is achieved by putting cold (sodium/cesium) atoms in a periodically pulsed standing wave of light [5]. Similarly, an experimental realization of our model could be achieved by putting cold atoms in a quasi-1D quantum dot. The atoms are then driven by a periodically pulsed standing wave of light. A quasi-1D quantum dot might be

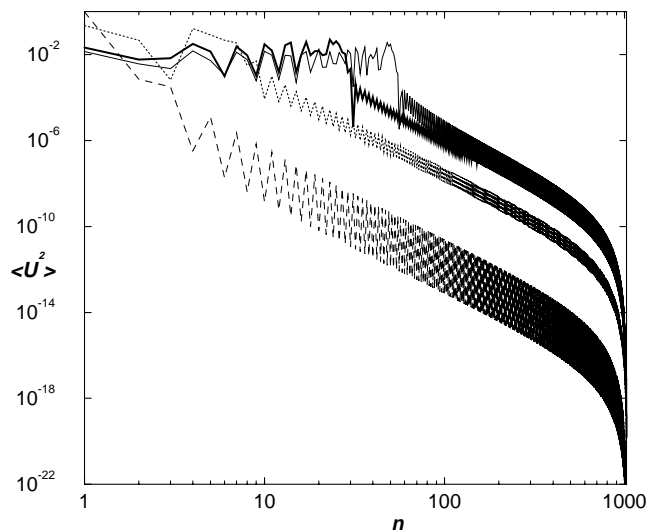


FIG. 4. The averaged matrix element $\langle U^2 \rangle$ versus n for different values of K . From left to right, the dashed curve for $K = 0.1$, dotted curve for $K = 5$, thick solid curve for $K = 25$, and thin solid curve for $K = 50$. The band width is about the order of K , which is clearly seen from the figure. The slopes of these four curves are about -4 .

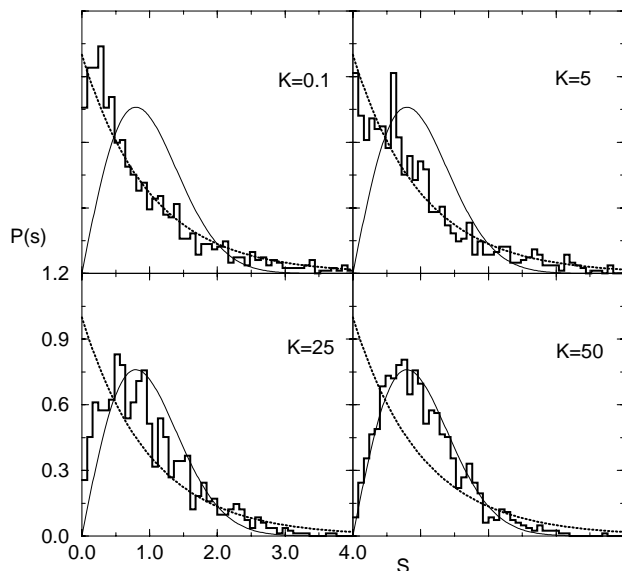


FIG. 5. The distribution of the nearest neighbor level spacing $P(s)$ for different values of K . The corresponding values of K are given in the figure. The dotted curve is Poisson and the thin curve is Wigner distribution. The histograms are numerical results. $P(s)$ at $K = 0.1$ and 5 are close to Poisson distribution and at $K = 25$ is intermediate, and $K = 50$ is close to Wigner distribution. The corresponding best fit Brody parameter β is 0.03, 0.08, 0.46, and 0.83, respectively.

formed by stretching a 2D quantum dot in one direction so that the length in one direction is much larger than the other. Such an experiment might allow us to study quantum chaos in a non-KAM system.

In summary, we have studied the classical and quantum behaviors of a kicked particle in a 1D infinite potential well. Despite its simplicity, our model exhibits a complicated stochastic web structure indicative of a non-KAM system. The classical dynamics is diffusive for any $K \neq 0$. For small K , the diffusion coefficient $D \propto K^{2.5}$, and for large K , $D \propto K^2$. The level statistics of quasideigenenergies shows a smooth transition from Poisson to Wigner distribution for a fixed dimension of the Floquet matrix. The quasideigenstates are found to be power-law localized with an exponent equal to two. Our model provides a new paradigm in the investigation of classical-quantum correspondence of stochastic motion in Hamiltonian systems with nonanalytic boundary conditions.

B. L. would like to thank F. Borgonovi, G. Casati, Y. Fyodorov, F. Izrailev, and A. Mirlin for helpful discussions. He also thanks the Abdus Salam International

Centre for Theoretical Physics (Trieste) for its kind hospitality during his visit there in the summer of 1998. The work was supported in part by grants from the Hong Kong Research Grants Council (RGC) and the Hong Kong Baptist University Faculty Research Grant (FRG).

- [1] G. Casati, B. V. Chirikov, J. Ford, and F. M. Izrailev, Lect. Notes Phys. **93**, 334 (1979).
- [2] B. V. Chirikov, Phys. Rep. **52**, 263 (1979); F. M. Izrailev, Phys. Rep. **196**, 299 (1990).
- [3] Special issue on quantum billiards [J. Stat. Phys. **83** (1995)].
- [4] E. J. Galvez, B. E. Sauer, L. Moorman, P. M. Koch, and D. Richards, Phys. Rev. Lett. **61**, 2011 (1988); J. E. Bayfield, G. Casati, I. Guarneri, and D. Sokol, *ibid.* **63**, 364 (1989).
- [5] F. L. Moore, J. C. Robinson, C. F. Bharucha, P. E. Williams, and M. G. Raizen, Phys. Rev. Lett. **73**, 2974 (1994).
- [6] F. Borgonovi, G. Casati, and B. Li, Phys. Rev. Lett. **77**, 4744 (1996); K. M. Frahm and D. L. Shepelyansky, *ibid.* **78**, 1440 (1997).
- [7] G. Casati, B. V. Chirikov, I. Guarneri, and F. M. Izrailev, Phys. Rev. E **48**, R1613 (1993); Phys. Lett. A **223**, 430 (1996).
- [8] M. El Ghafar, P. Törmä, V. Savichev, E. Mayr, A. Zeiler, and W. P. Schleich, Phys. Rev. Lett. **78**, 4181 (1997).
- [9] A. A. Chernikov, R. Z. Sagdeev, D. A. Usikov, M. Yu. Zakharov, and G. M. Zaslavsky, Nature (London) **326**, 559 (1987); A. A. Chernikov, R. Z. Sagdeev, and G. M. Zaslavsky, Physica (Amsterdam) **33D**, 65 (1988).
- [10] G. P. Berman, V. Yu. Rubaev, and G. M. Zaslavsky, Nonlinearity **4**, 543 (1991).
- [11] S. A. Gardiner, J. I. Cirac, and P. Zoller, Phys. Rev. Lett. **79**, 4790 (1997).
- [12] D. Shepelyansky and C. Sire, Europhys. Lett. **20**, 95 (1992); F. Borgonovi and L. Rebuzzini, Phys. Rev. E **52**, 2302 (1995); B. Hu, B. Li, J. Liu, and J.-L. Zhou, *ibid.* **58**, 1743 (1998).
- [13] F. Borgonovi, Phys. Rev. Lett. **80**, 4653 (1998); F. Borgonovi, P. Conti, D. Rebuzzini, B. Hu, and B. Li, Physica (Amsterdam) D (to be published).
- [14] W. H. Press, S. A. Teukolsky, W. T. Vetterling, and B. P. Flannery, *Numerical Recipes in Fortran* (Cambridge University Press, Cambridge, England, 1992).
- [15] A. M. Mirlin, Y. V. Fyodorov, F. M. Dittes, J. Quezada, and T. H. Seligman, Phys. Rev. E **54**, 3221 (1996).
- [16] T. A. Brody, J. Flores, J. B. French, P. A. Mello, A. Pandey, and S. S. M. Wong, Rev. Mod. Phys. **53**, 385 (1981).